NBS
Publi-
cations

NBS TECHNICAL NOTE 1073

U.S. DEPARTMENT OF COMMERCE / National Bureau of Standards

An Error Analysis for the Use of Presently Available Lunar Radio Flux Data in Broadbeam Antenna-System Measurements

NATIONAL BUREAU OF STANDARDS

The National Bureau of Standards[1] was established by an act of Congress on March 3, 1901. The Bureau's overall goal is to strengthen and advance the Nation's science and technology and facilitate their effective application for public benefit. To this end, the Bureau conducts research and provides: (1) a basis for the Nation's physical measurement system, (2) scientific and technological services for industry and government, (3) a technical basis for equity in trade, and (4) technical services to promote public safety. The Bureau's technical work is performed by the National Measurement Laboratory, the National Engineering Laboratory, and the Institute for Computer Sciences and Technology.

THE NATIONAL MEASUREMENT LABORATORY provides the national system of physical and chemical and materials measurement; coordinates the system with measurement systems of other nations and furnishes essential services leading to accurate and uniform physical and chemical measurement throughout the Nation's scientific community, industry, and commerce; conducts materials research leading to improved methods of measurement, standards, and data on the properties of materials needed by industry, commerce, educational institutions, and Government; provides advisory and research services to other Government agencies; develops, produces, and distributes Standard Reference Materials; and provides calibration services. The Laboratory consists of the following centers:

Absolute Physical Quantities[2] — Radiation Research — Chemical Physics — Analytical Chemistry — Materials Science

THE NATIONAL ENGINEERING LABORATORY provides technology and technical services to the public and private sectors to address national needs and to solve national problems; conducts research in engineering and applied science in support of these efforts; builds and maintains competence in the necessary disciplines required to carry out this research and technical service; develops engineering data and measurement capabilities; provides engineering measurement traceability services; develops test methods and proposes engineering standards and code changes; develops and proposes new engineering practices; and develops and improves mechanisms to transfer results of its research to the ultimate user. The Laboratory consists of the following centers:

Applied Mathematics — Electronics and Electrical Engineering[2] — Manufacturing Engineering — Building Technology — Fire Research — Chemical Engineering[2]

THE INSTITUTE FOR COMPUTER SCIENCES AND TECHNOLOGY conducts research and provides scientific and technical services to aid Federal agencies in the selection, acquisition, application, and use of computer technology to improve effectiveness and economy in Government operations in accordance with Public Law 89-306 (40 U.S.C. 759), relevant Executive Orders, and other directives; carries out this mission by managing the Federal Information Processing Standards Program, developing Federal ADP standards guidelines, and managing Federal participation in ADP voluntary standardization activities; provides scientific and technological advisory services and assistance to Federal agencies; and provides the technical foundation for computer-related policies of the Federal Government. The Institute consists of the following centers:

Programming Science and Technology — Computer Systems Engineering.

[1]Headquarters and Laboratories at Gaithersburg, MD, unless otherwise noted;
mailing address Washington, DC 20234.
[2]Some divisions within the center are located at Boulder, CO 80303.

An Error Analysis for the Use of Presently Available Lunar Radio Flux Data in Broadbeam Antenna-System Measurements

William C. Daywitt

Electromagnetic Fields Division
National Engineering Laboratory
National Bureau of Standards
U.S. Department of Commerce
Boulder, Colorado 80303

U.S. DEPARTMENT OF COMMERCE, Malcolm Baldrige, Secretary

NATIONAL BUREAU OF STANDARDS, Ernest Ambler, Director

Issued February 1984

National Bureau of Standards Technical Note 1073
Natl. Bur. Stand. (U.S.), Tech Note 1073, 35 pages (Feb. 1984)
CODEN: NBTNAE

U.S. GOVERNMENT PRINTING OFFICE
WASHINGTON: 1984

For sale by the Superintendent of Documents, U.S. Government Printing Office, Washington, DC 20402

CONTENTS

An Error Analysis for the Use of Presently Available Lunar Radio Flux Data in Broadbeam Antenna-System Measurements

W. C. Daywitt

National Bureau of Standards
Boulder, Colorado 80303

Simple, precise expressions for lunar diameter, average brightness temperature, flux density, and shape factor are presented. An analysis of the relationship between these parameters and corresponding errors are included. For broadbeam (HPBW>d) antennas, results show that flux density and shape factor can be determined with errors less than 13 percent and 0.4 percent respectively at frequencies below 10 GHz. Extension of the analysis to higher frequencies is indicated.

Key words: antenna temperature; error analysis; G/T; lunar flux density; shape factor.

1. Introduction

The antenna-system parameter G/T [1] can be directly measured by using the incoherent radiation from a radio star [2,3], thus circumventing difficulties associated with measuring G and T separately. Since the extraterrestrial sources used in the direct measurements function as noise power transfer standards, their flux densities and shape factors must be amenable to precise calibration. The angular diameter of the moon and its predictable output make it an appropriate source for the measurement of some antenna systems, and the purpose of this paper is to present results of an investigation into the potential accuracy of using the moon for these measurements.

The National Bureau of Standards (NBS) has been involved in G/T measurements since 1972 when it began a series [4,5] of studies concerning the use of some of the "brighter" sources, primarily Cassiopeia A, as precise transfer standards. Since that time it has developed [3,6,7,8] an earth-terminal-measurement-system for direct measurement of G/T and Satellite EIRP that operates off the IF patch panel of the receiving earth terminal. The measurement algorithms were developed for use on large (~ 18 m) antenna systems in the frequency range from 1 to 10 GHz, where a source the size of Cassiopeia A is appropriate. Recently NBS has performed successful measurements on a small

(~ 6 m) antenna system using the moon as a transfer standard for which the analysis presented here was completed.

Application of the lunar output to antenna and antenna-system measurements is not new. It has been used by radio astronomers [9,10] and communications engineers [11,12] alike, and the thermal radiation from its central region has been proposed as a radiometric standard for narrowbeam microwave and infrared observations [13]. The following presentation adds a detailed error analysis concerning the use of the radio output from the entire lunar surface as a standard for "broadbeam" (half-power beamwidth > lunar diameter) antennas that has previously been missing from the literature. The analysis was designed specifically for 1 to 10 GHz, although it will be clear from the presentation where it can be expanded outside this region. The main body of the text is a collection of simple but precise algorithms for calculating the lunar output and an accompanying summary of the error. For clarity, the more analytical aspects of the presentation are located in the appendices.

The receiver of an antenna system responds to the delivered power from its antenna waveguide terminal. This power is proportional to the antenna temperature [14] and is related to the radiation from a radio source in the antenna mainbeam by an equation of the form

$$T_a = C\, k_2\, S \tag{1}$$

where T_a is the antenna temperature, S is the flux density from the radio source, k_2 is a shape factor that accounts for variation of the source flux across the antenna beam pattern, and C is a factor containing system parameters unrelated to the lunar output. The equation indicates that an accurate calculation of T_a can only be made if both S and k_2 are accurately known. Consequently, in determining the usefulness of a particular radio source the accuracy with which the shape factor can be calculated must also be considered. Therefore, an analysis of the shape factor is included along with that of the flux density.

2. Lunar Flux Density and Average Brightness Temperature

An expression for the antenna temperature arising from a radio source in the antenna mainbeam is the starting point for a precise error analysis. From this expression follows those specifications (like frequency range or the ratio of half-power beamwidth to source diameter) that dictate under what conditions use of the chosen radio source will provide accurate results.

Because of its variation with lunar phase, the lunar flux density is best calculated as a function of the apparent lunar diameter and average brightness temperature. This function is derived in Appendix A and can be conveniently expressed as

$$S = 7.349\, f^2\, \bar{T}\, d^2 \tag{2}$$

where S is the flux density in Janskys (10^{-26} watts/Hz/meter^2), f is the measurement frequency in GHz, $\bar{T}$ is the average lunar brightness temperature in kelvins, and d is the angular diameter of the moon in degrees subtended at the antenna site. This diameter can be easily calculated from eq (B2) in Appendix B with an error less than ±0.1 percent.

Disregarding errors in f, $\bar{T}$, and d, eq (2) is an approximation (Appendix A) which is accurate to ±4.34 percent. It appears that this error could be reduced to ±1 percent if the yearly variation in the solar insolation at the lunar surface due to the earth's eccentric orbit were taken into account.

An expression for the average brightness temperature that contains effects of lunar phase can be written in the form [9]

$$\bar{T} = \bar{T}_0 \left[1 - \left(\frac{\bar{T}_1}{\bar{T}_0}\right) \cos(\phi - \Psi) \right] \tag{3}$$

where $\bar{T}_0$, $(\bar{T}_1/\bar{T}_0)$, and the phase lag Ψ are functions of frequency that can be determined from radio measurements. ϕ is the lunar phase angle ($\phi = 0°$ at new moon) which is related [15] to the phase (fraction F of the apparent lunar disk illuminated by the sun) through the equation

$$\phi = \arccos(1 - 2F). \tag{4}$$

F can be obtained from The Astronomical Almanac [16] to an accuracy of ±2 percent by a simple parabolic fit over a three-day period. This leads to a maximum error in $\cos\phi$ of 0.04 and a negligible error in $\bar{T}$. Disregarding errors in the parameters appearing in eq (3), the error (Appendix D) in $\bar{T}$ due to retaining only the fundamental ϕ on the right-hand side of the equation is ±0.18 percent.

The value of eq (3) lies in the fact that with it the average brightness temperature $\bar{T}$ can be calculated for any lunar phase, leaving only three parameters, $\bar{T}_0$, $(\bar{T}_1/\bar{T}_0)$, Ψ, to be accurately measured at a few frequencies and extrapolated in between. This process will be illustrated in the remainder of the section for 1 to 10 GHz with data taken from the literature [9] and reproduced in table 1.

Table 1. Parameters for the average lunar brightness temperature

Frequency (GHz)	$\bar{T}_0$(kelvins)	$\bar{T}_1/\bar{T}_0$	Ψ(degree)	T_1/T_0
0.6	240	--	--	--
0.86	235	--	--	--
1.5	225	0.00667	44	0.00800
3.13	218	0.0183	42	0.0204
9.375	210	0.0619	40	0.0681
18.75	207	0.155	35	0.151
37.5	205	0.195	32	0.217
75	203	0.266	24	0.326

The values in table 1 for $\bar{T}_0$ are quoted with accuracies from 5 to 10 percent, although with more recent measurement techniques [5,17,18] they could all be determined to approximately 5 percent. The accuracies of the ratios $\bar{T}_1/\bar{T}_0$ and T_1/T_0 are quoted to 2 percent, and the phase lag Ψ to 10° for frequencies below 15 GHz, and 5° for frequencies above. Figures 1, 2, 3, and 4 were plotted from these data.

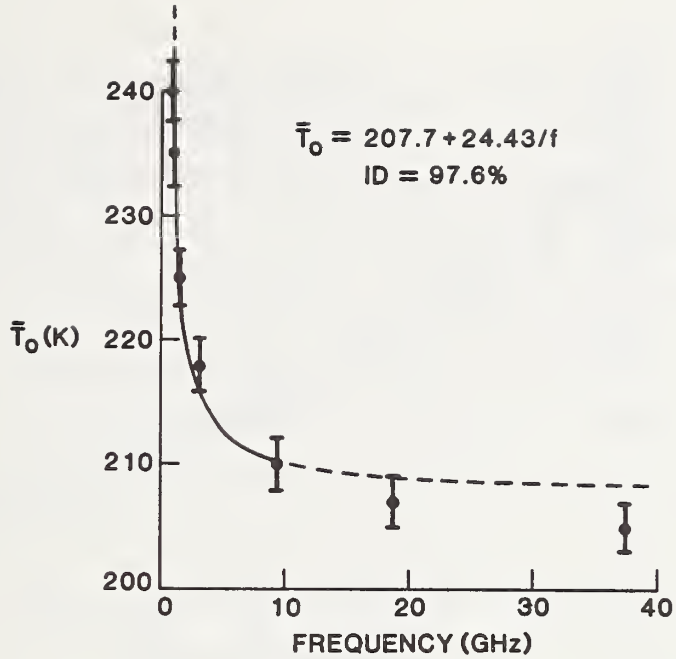

Figure 1. Constant term versus frequency for the average brightness temperature.

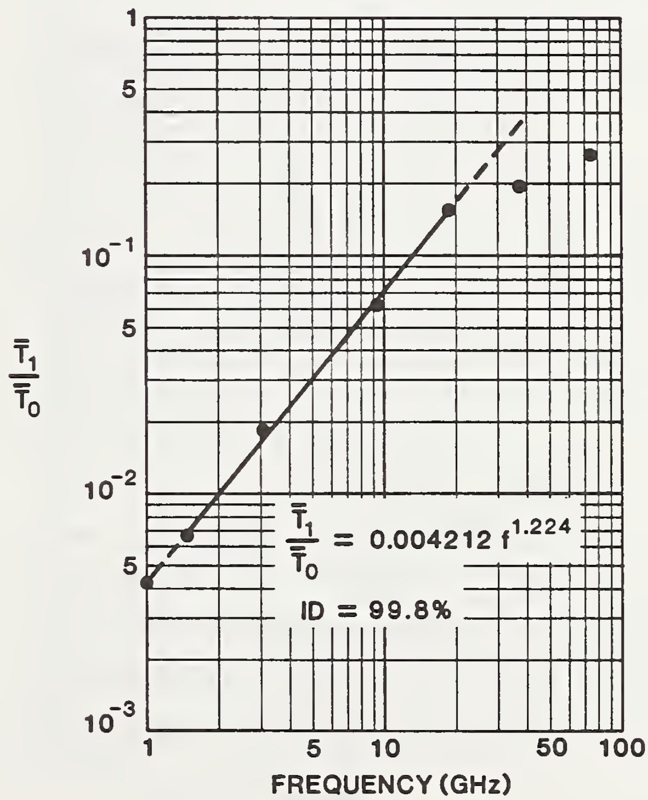

Figure 2. First-harmonic ratio versus frequency for the average brightness temperature.

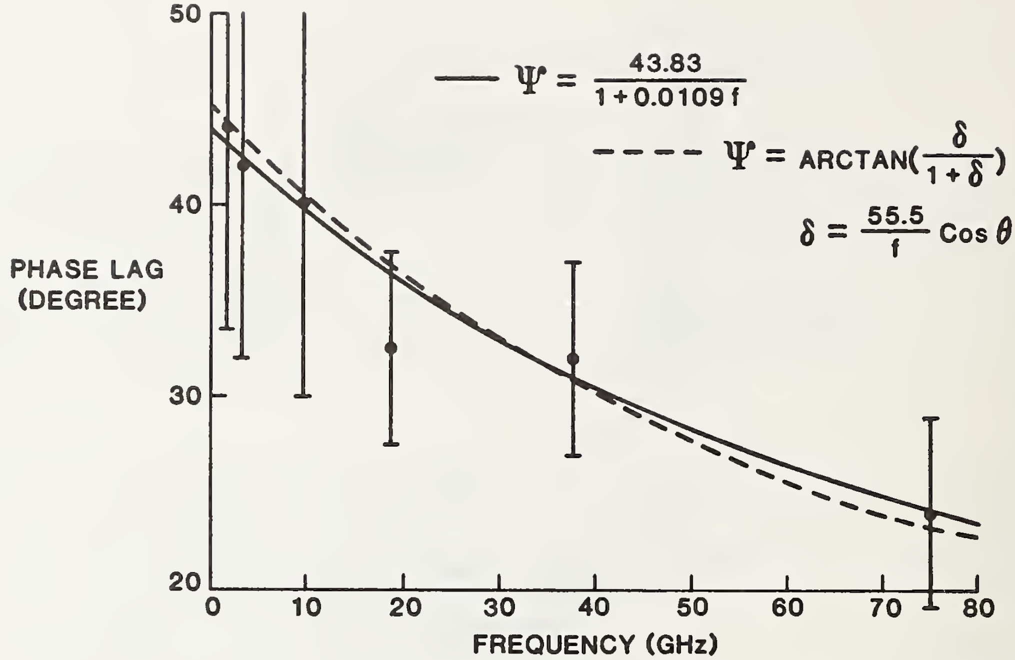

Figure 3. Phase lag versus frequency for the first harmonic of the average brightness temperature.

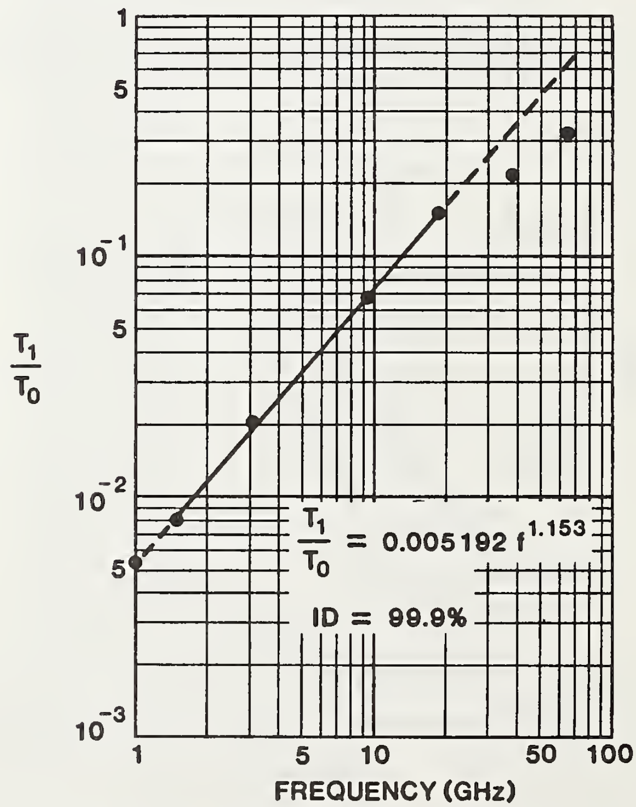

Figure 4. First-harmonic ratio versus frequency for the subterrestial brightness temperature.

Figure 1 shows the constant term, $\bar{T}_0$, of the average brightness temperature with 10 percent error bars plotted as a function of frequency. Assuming a radio absorption coefficient proportional to frequency [13] and independent of depth into the lunar soil, $\bar{T}_0$ is linear in inverse frequency. This functional form is least-squares fit to the data from 0.86 to 18.75 GHz with the resulting formula shown in the figure. The index of determination [19], denoted by ID in the figure, indicates that 97.6 percent of the variance shown in the data is explained by the form of $\bar{T}_0$. The largest difference between the curve and the fitted data from 1 to 10 GHz is 1.4 percent. Combining this with a 5 percent achievable error (not the 10 percent error bars shown) in the data indicates that it is possible to determine $\bar{T}_0$ to ±6.4 percent.

The data for $\bar{T}_1/\bar{T}_0$ from column 3 of table 1 is plotted in figure 2. The points from 1.5 to 18.75 GHz were least-squares fit with a power-law curve, resulting in a 99.8 percent index of determination. A maximum error of 4.6 percent between these points and the curve is obtained. Combining this error with the 2 percent quoted for the ratio leads to an error of 6.6 percent when using the formula shown in the figure. This gives a maximum error of ±0.46 percent for $\bar{T}$ in the 1 to 10 GHz range.

Figure 3 is a plot of the phase lag with the error limits associated with table 1. The "arctan" curve is used in Appendix C and is of no concern now. The least-squares curve that is calculated from the formula shown has an index of determination of 99.1 percent. It is within 2° of the data from 1 to 10 GHz, and combined with the error bars leads to an error of 12° in that region. This leads to a maximum error of ±1.22 percent for $\bar{T}$.

The previous systematic error components are collected in table 2. It should be remembered that the 5 percent error for $\bar{T}_0$ represents an achievable error, and should not be applied in practice to all of the data in column 2 of the table. Table 2 shows a maximum 12.8 percent linear sum of errors which is acceptable for G/T measurements.

Table 2. Summary of systematic flux density errors from 1 to 10 GHz

Source of Error	Magnitude	Resulting % Error in S
Variation in Solar Insolation (Appendix B)	3.34% + 1%	4.34
Neglect of Higher Harmonics in Eq (D3) (Appendix D)	0.18%	0.18
$\bar{T}_o$	5% + 1.4%	6.4
$\bar{T}_1/\bar{T}_o$	6.6%	0.46
$\cos\phi$	0.04	0.00
Ψ	12°	1.22
d	0.1%	0.2
Quadrature Sum		±7.8% (0.33 dB)
Linear Sum		±12.8% (0.52 dB)

3. Shape Factor

The shape factor k_2 in eq (1) approaches unity as the ratio of the antenna half-power beamwidth (HPBW) to lunar diameter increases without limit. For finite ratios it may be calculated from [5]

$$k_2 = \frac{1 - e^{-x^2}}{x^2} \tag{5}$$

where

$$x^2 \equiv 0.6441(d/\theta_H)^2 , \tag{6}$$

and where d and θ_H are the apparent (or optical) angular diameter of the moon (Appendix B) and antenna HPBW respectively. Disregarding errors in d or θ_H, the approximations leading to eq (5) (Appendix C) generate an error no larger than ±0.32 percent in k_2 for θ_H/d greater than unity and a frequency less than than 10 GHz.

Taking the total differential of k_2 will give an estimate of the errors in k_2 due to errors in d and θ_H. From Appendix B the error in d is ±0.1 percent. The error due to θ_H depends upon the scheme used in viewing the moon. In at least one scheme [3] the systematic error vanishes, and hence will be taken to be zero here. Performing the differential leads to a ±0.06 percent error in k_2 due to the ±0.1 percent lunar diameter error. Thus, the total error in k_2 from using eq (5) is ±0.38 percent (0.32 + 0.06) for θ_H/d greater than unity and frequencies less than 10 GHz.

4. Conclusions

The lunar flux density and shape factor can be easily calculated for any lunar phase and earth-moon separation distance using both the equations presented and The Astronomical Almanac [16]. The maximum systematic errors for the flux density and shape factor are ±13 percent and ±0.4 percent respectively for broadbeam ($\theta_H > d$) antennas in the 1 to 10 GHz frequency range. This flux-density error could be reduced from ±13 percent to ±10 percent by taking the variable solar insolation into account. The regression equations shown in figures 1, 2, and 3 are of course somewhat arbitrary and could be replaced by other forms.

The small value (±0.18 percent) of the "higher-harmonic" error in table 2 indicates that the analysis can readily be extended to higher frequencies, but a frequency will ultimately be reached where the simple form of eq (3) will have to be replaced with one containing harmonics of the fundamental ϕ. Unfortunately, data like that in table 1 does not exist for these harmonics.

5. Acknowledgments

The author wishes to thank M. Kanda, D. F. Wait, and a number of other of his colleagues in the Electromagnetic Fields Division of NBS for many helpful and stimulating discussions.

6. References

[1] Altman, F. J.; Burgess, J. L.; Driscoll, C. R.: McAllister, N. F.; Selz, G. O.; Tunstall, B.; Young, H. M. Satellite communications reference data handbook. Defense Communications Agency. Report No. AD-746165, distributed by NTIS, U.S. Department of Commerce; 1972 July.

[2] Kreutel, Jr., R. W.; Pacholder, A. O. The measurement of gain and noise temperature of a satellite communications earth station. Microwave Journal. 12(10); 1969 October.

[3] Wait, D. F. Satellite earth terminal G/T measurements. Microwave Journal. 20(4); 1977 April.

[4] Wait, D. F.; Daywitt, W. C.; Kanda, M.; Miller, C. K. S. A study of the measurement of G/T using Cassiopeia A. Nat. Bur. Stand. (U.S.) NBSIR 74-382; 1974 June.

[5] Kanda, M. An error analysis for absolute flux density measurements of Cassiopeia A. IEEE Trans. Instr. Meas. IM-25(3): 173; 1976 September.

[6] Daywitt, W. C. Error equations use in the NBS precision G/T measurement system. Nat. Bur. Stand. (U.S.) NBSIR 76-842; 1976 September.

[7] Daywitt, W. C. An error analysis for the measurement of satellite EIRP using a calibrated radio star. IEEE Trans. Instr. Meas. IM-27(3): 253; 1978 September.

[8] Daywitt, W. C. Atmospheric propagation equations used in the NBS earth terminal measurement system. Nat. Bur. Stand. (U.S.) NBSIR 78-883; 1978 April.

[9] Kuz'min, A D.; Salomonovich, A. E. Radioastronomical methods of antenna measurements. New York, London: Academic Press; 1966.

[10] Baars, J. M. W. The measurement of large antennas with cosmic radio sources. IEEE Trans. A. P. AP-21(4): 461; 1973 July.

[11] Johannsen, K. G.; Koury, A. The moon as a source for G/T measurements. IEEE Trans. A. ES.: 718; 1974 September.

[12] Saam, T. J. Small computers revolutionize G/T tests. Microwaves. 37; 1980 August.

[13] Linsky, J. L. The moon as a proposed radiometric standard for microwave and infrared observations of extended sources. The Astrophysical Journal. Supp. Ser. 25(216): 163; 1973 February.

[14] Kraus, J. D.; Tiuri, M. E. Radio astronomy. New York: McGraw-Hill; 1966.

[15] Explanatory supplement to the astronomical ephemeris and the American ephemeris and nautical almanac. London: H. M. Nautical Almanac Office, Her Majesty's Stationery Office; 1961.

[16] The astronomical almanac for the year 1981. Nautical Almanac Office of the U.S. Naval Observatory; 1981.

[17] Kanda, M. Accuracy considerations in the measurement of the power gain of a large microwave antenna. IEEE Trans. A. P. 407; 1975 May.

[18] Kerns, D. M. Plane-wave scattering-matrix theory of antennas and antenna-antenna interactions. Nat. Bur. Stand. (U.S.) Monogr. 162; 1981 June.

[19] Crow, E. L.; Davis, F. A.; Maxfield, M. W. Statistics manual. U.S. Naval Ordnance Test Station; 1955.

[20] Ko, H. C. Antenna temperature and the temperature of electromagnetic radiation. IEEE Trans. A. P. 126; 1964 January.

[21] Soboleva, N. S. Measurement of the polarization of lunar radio emission on a wavelength of 3.2 cm. Soviet Astronomy-AJ. 6(6): 873, 1963 May.

[22] Krotikov, V. D.; Troitskii, V. S. Radio emission and nature of the moon. Soviet Physics Uspekhi. 6(6): 841; 1964 May.

[23] Allen, C. W. Astrophysical quantities. Univ. of London: The Athlone Press; 1976.

[24] Labs, D.; Neckel, H. The solar constant. Solar Physics. 19: 3; 1971.

[25] Baars, J. W. M.; Mezger, P.G.; Wendker, H. The spectra of the strongest non-thermal radio sources in the centimeter-wavelength range. The Astrophysical Journal. 142(1); 1965 July.

[26] Linsky, J. F. Models of the lunar surface including temperature-dependent thermal properties. ICARUS 5: 606; 1966.

[27] Muhleman, D. O. Microwave emission from the moon. Lucus, J. W., ed. Thermal characteristics of the moon. Progress in Astronautics and Aeronautics Ser. 28; 1972.

[28] Salomonovich, A. E. Thermal radio emission of the moon and certain characteristics of its surface layer. Kopal, Z.; Mikhailov, Z. K. ed. The moon. London, New York: Academic Press; 1962.

APPENDIX A

DERIVATION OF A USEFUL RELATIONSHIP BETWEEN LUNAR FLUX DENSITY AND AVERAGE BRIGHTNESS TEMPERATURE

The antenna temperature [14] corresponding to the power available from the antenna waveguide port is measured by the antenna system. Consequently, it is with this quantity that an analysis must start, relating other measurement variables to it. The antenna temperature T_a corresponding to lunar radiation in the antenna mainbeam can be written as

$$T_a = T_a(\Omega,\phi,g) = \frac{\eta}{\Omega_a} \int MTP_n d\Omega \tag{A1}$$

where [14,20]

$$M = 1 + \left(\frac{T' - T''}{T' + T''}\right) \cos 2\varepsilon_a \cos 2(\tau - \tau_a) \tag{A2}$$

and

$$T \equiv \frac{T' + T''}{2} . \tag{A3}$$

The antenna temperature is a function of the relative earth-moon geometry through the solid angle Ω subtended by the moon at the antenna, the lunar phase angle ϕ, and the solar mean anomaly g [15]. The latter dependance results from variable solar insolation caused by the eccentricity of the earth's orbit. η, Ω_a and P_n are the antenna radiation efficiency, solid angle, and normalized power pattern, respectively. M is a factor describing the mismatch between the moon's radial polarization [21] and the antenna polarization, with the angles ε_a, τ_a and τ defined on the Pointearé sphere

[14]. $d\Omega$ is the differential solid angle subtended by a small portion of the lunar surface as seen from the antenna position on the earth. T' and T" are radial and azimuthal (with respect to the subterrestial point on the lunar surface) brightness temperatures of the lunar surface, with the radial componant T' being the principle or strongest of the two. The quantity (T' - T")/(T' + T") is the degree of polarization and varies from zero at the subterrestial point to a maximum at the lunar limbs.

Depending on the frequency and elevation angle, atmospheric attenuation can significantly reduce the magnitude of T_a. Nevertheless, this effect has been deliberately left out of eq (A1) in order to focus attention upon the flux density and shape factor calculations.

Equation (A1) can be reduced to a more convenient form in a strictly formal way, resulting in the equation

$$T_a = \frac{\eta}{\Omega_a} k_2 \ k_6 \ \Omega \ \frac{\int T d\Omega}{\Omega} \tag{A4}$$

with the definitions

$$k_2 = k_2(\Omega,\phi,g,\theta_H) \equiv \frac{\int TP_n d\Omega}{\int T d\Omega} \tag{A5}$$

$$k_6 = k_6(\Omega,\phi,g,\theta_H) \equiv \frac{\int MTP_n d\Omega}{\int TP_n d\Omega} \tag{A6}$$

$$\Omega \equiv \text{total lunar solid angle} \doteq \frac{\pi d^2}{4} . \tag{A7}$$

d is the lunar angular diameter (Appendix B), k_2, and k_6 are the shape and polarization factors [5] respectively, and θ_H is the antenna half-power beamwidth. The reason for defining these factors stems from the fact that under certain conditions they can be easily and accurately approximated, and help reduce the equation for T_a to a usable form. The shape factor k_2 is discussed in Appendix C. The last ratio in eq (A4) is a function of Ω, ϕ, g and represents an average brightness temperature $\bar{T}(\Omega,\phi,g)$. However, defining this ratio as the lunar brightness temperature incorporates the earth-moon geometry (through the presence of Ω) in the definition, an undesirable feature that can be eliminated by continuing the formal development a little bit further:

$$\frac{\int T d\Omega}{\Omega} = \bar{T}(\Omega,\phi,g) = \partial \bar{T}' \ , \tag{A8}$$

where

$$\partial = \partial(\Omega,\phi,g) \equiv \frac{\bar{T}(\Omega,\phi,g)}{\bar{T}(\phi,g)} \tag{A9}$$

and

$$\bar{T}' \equiv \bar{T}(\phi,g) \equiv \frac{\int T d\Omega}{\partial\Omega} \ . \tag{A10}$$

$\bar{T}'$ is the average brightness temperature, and is a function of lunar phase and solar mean anomaly. Its usefulness results from the fact that ∂ is close to unity. A model for $\bar{T}'$ has been developed [22] that reasonably fits the experimental data [9] as a function of frequency and lunar phase ϕ, although no attempt was made in the literature to account for the variable solar insolation indicated by the presence of g in eq (A10). In accounting for this effect it is convenient to make one more formal manipulation:

$$\bar{T}(\phi,\pi/2) = \sigma(\phi,g)\bar{T}' \tag{A11}$$

where

$$\sigma(g) \equiv \frac{\bar{T}(\phi,\pi/2)}{\bar{T}(\phi,g)} \tag{A12}$$

$\pi/2$ (or $3\pi/2$) is the solar mean anomaly where the earth-sun separation distance is equal to 1 astronomical unit (1 Au = the average earth-sun separation distance [23]). Consequently, $\bar{T}(\phi,\pi/2)$ is $\bar{T}'$ normalized to 1 Au. The normalization factor σ is not strongly dependent upon lunar phase and, consequently the phase doesn't appear in the argument of σ. It will be seen shortly that the error in $\bar{T}'$ from neglecting the variable solar flux can be as high as ±3.34 percent, so it would be of value to use the normalized brightness temperature in future spectral characterizations such as the one in table 1.

The earth-sun separation distance R in astronomical units is given by [16]

$$R = 1 - 0.0167 \cos g \tag{A13}$$

where the quantity (0.0167) is the eccentricity of the earth's orbit about the sun. The mean anomaly g in degrees is easily calculated from [16]

$$g = 357.0 + 0.9856D \tag{A14}$$

where D is the yearly day number [16], to an accuracy sufficient for eq (A13) and those to follow. The solar insolation at the lunar surface is proportional to R^2, hence the temperature of the lunar soil varies throughout the year. Since the variation is slow relative to a synodic period, it appears that the perturbing effect on the linear approximations of the lunar heat and radiation equations can be treated quasi-statically, leading to an average temperature T_o of the form

$$T_o = T_{oo}(1 + 0.0334 \cos g) \tag{A15}$$

where T_{oo} is the average temperature T_o at 1 Au. Equation (A15) leads to a normalizing factor of the form

$$\sigma(g) = 1 - 0.0334 \cos g \quad . \tag{A16}$$

The preceding development of σ assumes a constant solar output. However, according to available data possible variations in the solar constant with amplitudes up to ±1 percent cannot be ruled out [24]. Furthermore, no final conclusions can be drawn at this time about possible correlations to other solar phenomena [24], making easy detection of a change in the solar constant difficult.

The parameter ∂ in eq (A9) was estimated using the brightness temperature of eq (C4) with the small variable term removed, and yielded a value equal to the quantity $(1 + 0.013d)$. With a lunar diameter d of 0.5°(0.0087 radians), ∂ is only 0.01 percent greater than unity, implying that for the earth-moon separation distance the lunar output is well represented by an average brightness that is a property only of the lunar surface and not the relative earth-moon geometry.

The brightness temperature given by eq (C4) was used to estimate the polarization factor k_6. The largest deviation from unity for any lunar phase or antenna polarization over the 1 to 10 GHz range was found to be 0.1 percent, showing that k_6 can be dropped with little error.

Equation (A4) can now be written as

$$T_a = \frac{\eta}{\Omega_a}\left(\frac{\lambda^2}{2k}\right) k_2 \; S \pm 0.1\% \pm 0.01\% \qquad \text{(A17)}$$

where the first error (±0.1 percent) comes from setting k_6 equal to unity and the second (±0.01 percent) from setting ∂ equal to unity. k is Boltzmann's constant and λ is the measurement wavelength. The flux density S in eq (A17) becomes

$$S = \left(\frac{2k}{\lambda^2}\right) \bar{T}'\Omega \pm 1\% \qquad \text{(A18)}$$

$$= \left(\frac{2k}{\lambda^2}\right) \bar{T}\Omega \pm 1\% \pm 3.34\% \qquad \text{(A18')}$$

where the first error (±1 percent) comes from a possible variation in the solar constant and the second (±3.34 percent) from the variable solar insolation due to the earth's eccentric orbit. The $\bar{T}$ appearing in (A18') and eq (2) of Section 2 corresponds to that of eq (A8), thus leading to the additional ±3.34 percent error. Equation (A18') is the starting point for Section 2.

APPENDIX B

ANGULAR LUNAR DIAMETER

The apparent lunar diameter as seen by an observer on the earth's surface can be deduced from the earth-moon geometry shown in figure 5, where d is the average lunar angular diameter, r_m is the average lunar radius, r_0 is the geocentric earth-moon separation, a is the equatorial radius of the earth, LAT is the latitude of the observer, r_e is the geocentric radius to the observer's "sea level" and is a function of his latitude [15], z is the observer's altitude above sea level, and el is the elevation angle to the lunar center. The angular diameter is related to the other parameters by the equation

$$d = 2 \text{ arc sin} \left\{ \frac{r_m}{[r_o^2 - (r_e + z)^2 \cos^2 el]^{1/2} - (r_e + z) \sin el} \right\} . \qquad \text{(B1)}$$

After dividing the numerator and denominator of this expression by the earth's equatorial radius and performing a number of approximations, the following equation for d in degrees is obtained:

$$d = \frac{0.5182}{(r_o/a)/60.268 - 0.0166 \sin el} . \qquad \text{(B2)}$$

The angular diameter is now only a function of the earth-moon distance and the elevation angle at the time of observation. The quantity "60.268" is the mean earth-moon distance in units of the earth's equatorial radius. The ratio r_0/a can be obtained from The Astronomical Almanac [16] at the beginning (midnight) of each day of the year to an accuracy of 0.002 percent, and a simple parabolic extrapolation including the values for three consecutive days gives a result accurate to 0.02 percent. The approximations leading to eq (B2) add up to a total error of 0.1 percent in calculating the lunar diameter from this equation.

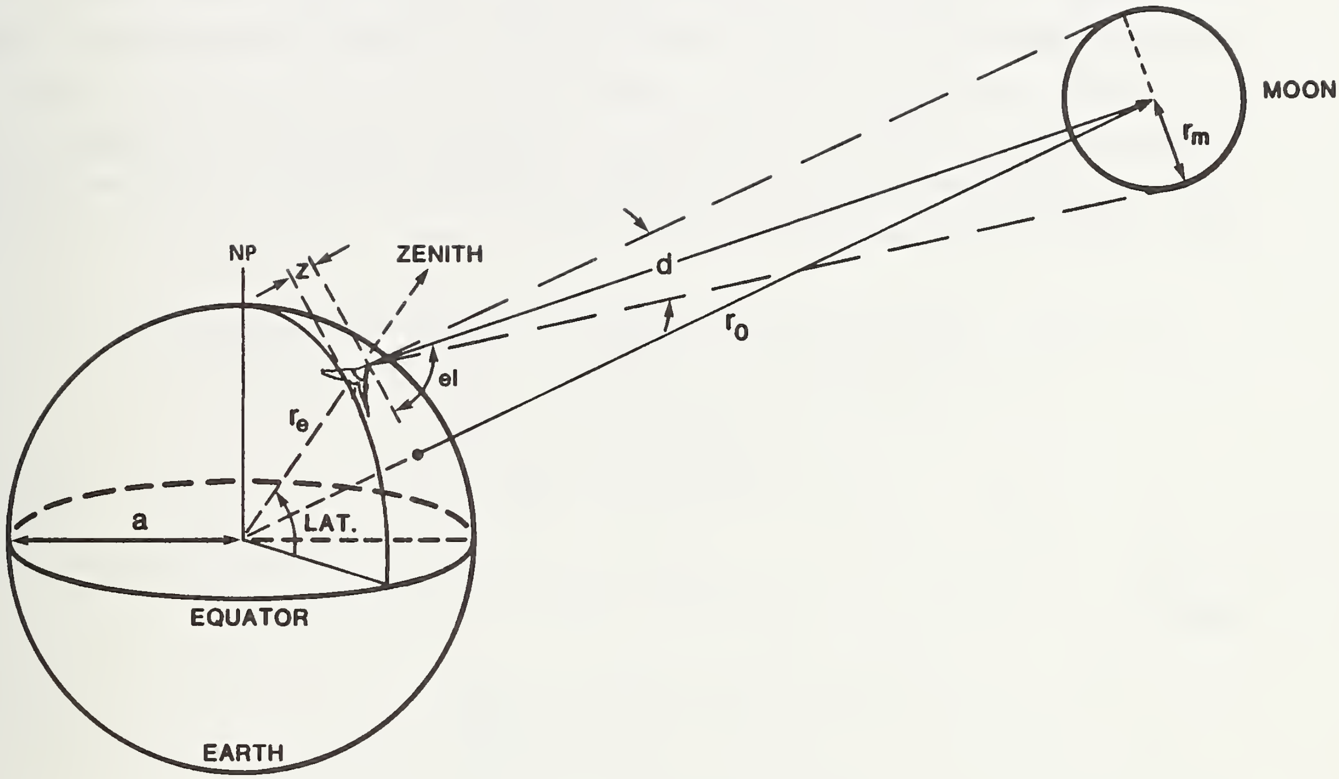

Figure 5. Relative earth-moon geometry.

APPENDIX C

A DISK MODEL FOR THE LUNAR SHAPE FACTOR

The effect of an antenna power pattern upon the antenna temperature T_a is contained in the convolution integral of eq (A5). Under favorable conditions, the resulting shape factor k_2 can be accurately reduced to a simple expression containing only the ratio d_e/θ_H, where d_e is an effective lunar diameter and θ_H is the antenna HPBW. Radio astronomers [25] first used a simple disk model with a constant brightness temperature to describe the output of Casseopia A, which was later refined [5] by choosing the effective diameter to minimize the error from using such a simple model.

The shape factor described by eq (A5) can be formally written as

$$k_2 \equiv \frac{\int TP_n d\Omega}{\int T d\Omega} = \left(\frac{1 - e^{-x^2}}{x^2}\right) I \tag{C1}$$

where

$$x^2 \equiv (\ln 2)\,(d_e/\theta_H)^2 \tag{C2}$$

and

$$I = I(\Omega,\phi,g,\theta_H) \equiv \left(\frac{x^2}{1 - e^{-x^2}}\right)\frac{\int TP_n d\Omega}{\int T d\Omega} \quad . \tag{C3}$$

The first factor in eq (C1) is the shape factor for a disk of constant brightness. If I were deleted from this equation, the ratio (1 - I)/I becomes the relative error in using a disk model to estimate k_2. The effective diameter will be chosen to minimize this error for θ_H/d greater than unity.

The integrals in eq (C3) require some knowledge of the normalized antenna power pattern P_n and the lunar surface brightness temperature. If these quantities were known with sufficient accuracy, T_a could be calculated directly from eq (A1). Although this is not the case, it is often possible to approximate the power pattern inside the HPBW by a Gaussian function--sometimes even down to the -10dB point on the pattern. Defining the pattern width at the -10dB point to be the maximum usable source diameter d leads to a specification of 0.55d as the narrowest HPBW that should be measured using the source.

A model of the surface brightness temperature T that is quite adequate for estimating the error in setting I equal to unity can be obtained from the literature [22, 26, 27]. The model used in the calculations is

$$T = T(\alpha,\beta,\phi) = \varepsilon\, T_o \left\{ 1 - \left(\frac{T_1}{T_o}\right) \frac{\cos(\phi + \Delta\phi - \Psi)}{(1 + 2\delta + 2\delta^2)^{1/2}} \right\} \cos^{1/2} \psi \qquad \text{(C4)}$$

where

$$\varepsilon = \varepsilon(\theta_o) = \varepsilon_{\parallel}(\theta_o) + \varepsilon_{\perp}(\theta_o) \qquad \text{(C5)}$$

$$2\varepsilon_{\parallel} = 1 - \left[\frac{\cos\theta_o - (\varepsilon' - \sin^2\theta_o)^{1/2}}{\cos\theta_o + (\varepsilon' - \sin^2\theta_o)^{1/2}} \right]^2 \qquad \text{(C6)}$$

$$2\varepsilon_{\perp} = 1 - \left[\frac{\varepsilon'\cos\theta_o - (\varepsilon' - \sin^2\theta_o)^{1/2}}{\varepsilon'\cos\theta_o + (\varepsilon' - \sin^2\theta_o)^{1/2}} \right]^2 \qquad \text{(C7)}$$

$$\Psi = \Psi(\theta) = \text{arc tan}\left(\frac{\delta}{1 + \delta}\right) \qquad \text{(C8)}$$

and

$$\delta = \delta(\theta) = \delta_1 \cos\theta \quad . \qquad \text{(C9)}$$

With reference to figure 6, T is the surface brightness temperature with selenographic coordinates $\Delta\phi$ and ψ which correspond to the coordinates α and β in the observer's coordinate frame on the earth's surface. ϕ is the lunar phase angle for which I is calculated. The integrals in eq (C3) are performed over the entire apparent solid angle of the surface with $d\Omega$ as the corresponding differential. ε is the surface emissivity and is composed of a part $\varepsilon_{\parallel}$ associated with radiation parallel to the plane of incidence defined by the points e, m, and the surface point, and a part $\varepsilon_{\perp}$ perpendicular to that plane. ε' is an average dielectric constant set equal to 1.64 [9] for the calculations. The angles, θ_0 and θ, are related to each other by Snell's law and to α and β through the geometry shown in the figure. T_0 is a constant thermal temperature resulting from solar heating, and T_1 is the corresponding fundamental harmonic amplitude. Ψ is the phase lag between initial solar heating and subsequent radio emission. δ_1 is the ratio of the thermal absorption coefficient to the radio absorption coefficient.

In the calculation of I, it can be seen from the ratio of the integrals in eq (C3) that the constant T_0 in eq (C4) will drop out and need not be considered. This leaves the ratio (T_1/T_0) and the parameter δ_1 to be determined. The data [9] plotted in figure 4 was least-squares fit between 1 and 20 GHz with a straight line, resulting in the formula for (T_1/T_0) shown in the figure. The value of δ_1 that was used to calculate I was obtained by making it proportional to inverse frequency, and fitting the resulting phase lag Ψ to the data in figure 3.

As a check on the model for T, calculations from the model were compared to measurements of the surface brightness temperature at 9.375 GHz [28]. Figures 7 and 8 show the results for the two lunar phases 168° and 262° respectively. An equatorial and a polar profile of the brightness are shown in both figures with the experimental data plotted with solid lines. The dashed lines, resulting from the model calculations, were shifted upwards for clarity.

Figure 9 shows the error (1 - I)/I at 9.375 GHz and 168° for different values of the effective diameter d_e. Both the half-power beamwidth and the effective diameter are normalized by the apparent lunar diameter d. The

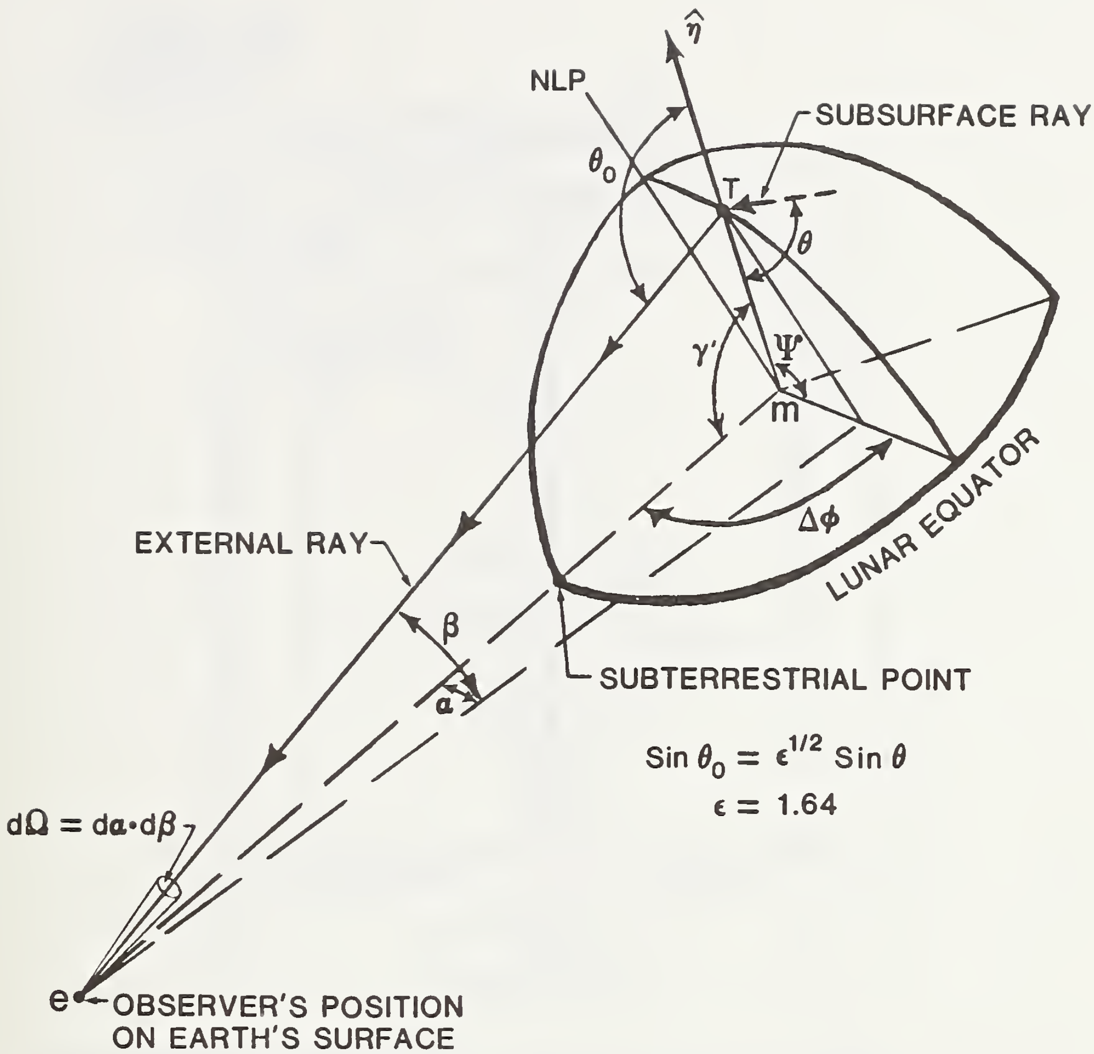

Figure 6. Pictorial relationship between observer and lunar coordinates.

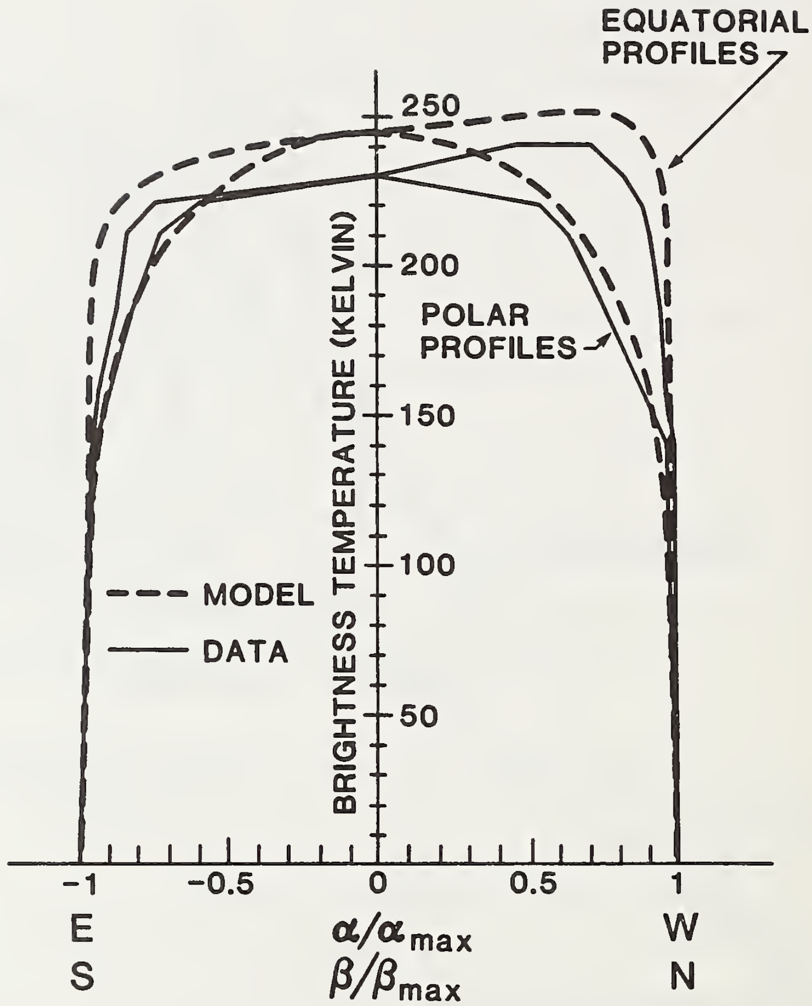

Figure 7. Comparison at 168° and 9.375 GHz between calculated and measured profiles of the brightness temperature.

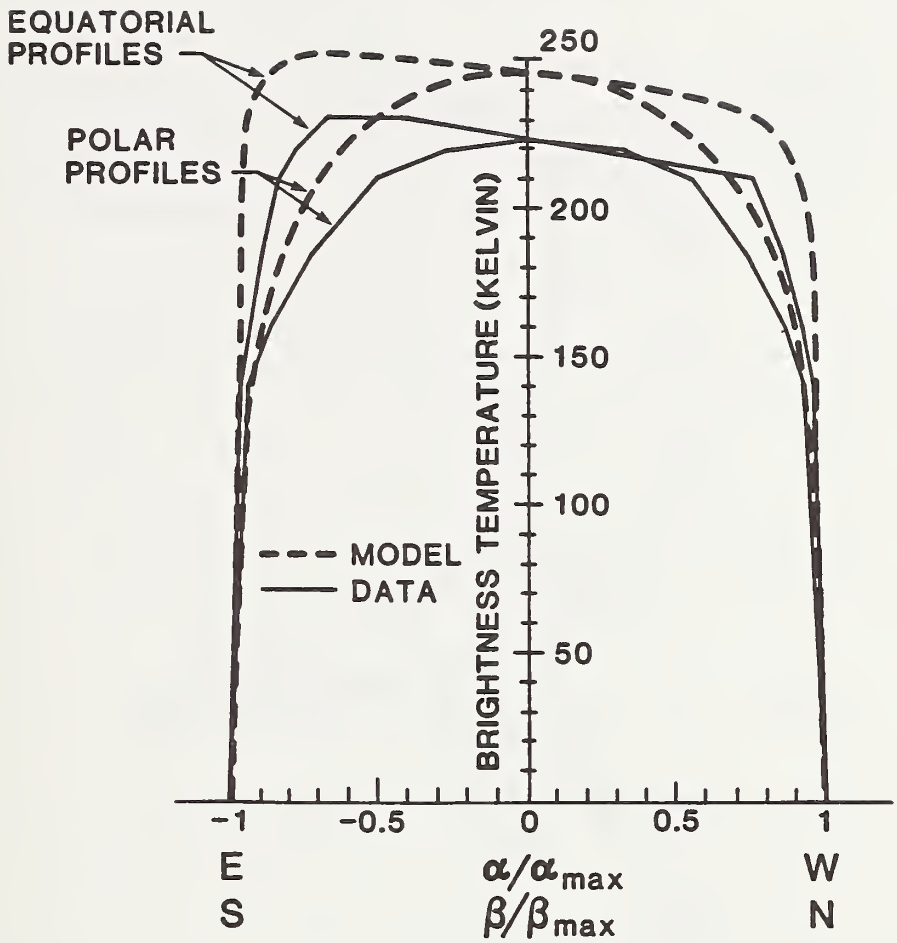

Figure 8. Comparison at 262° and 9.375 GHz between calculated and measured profiles of the brightness temperature.

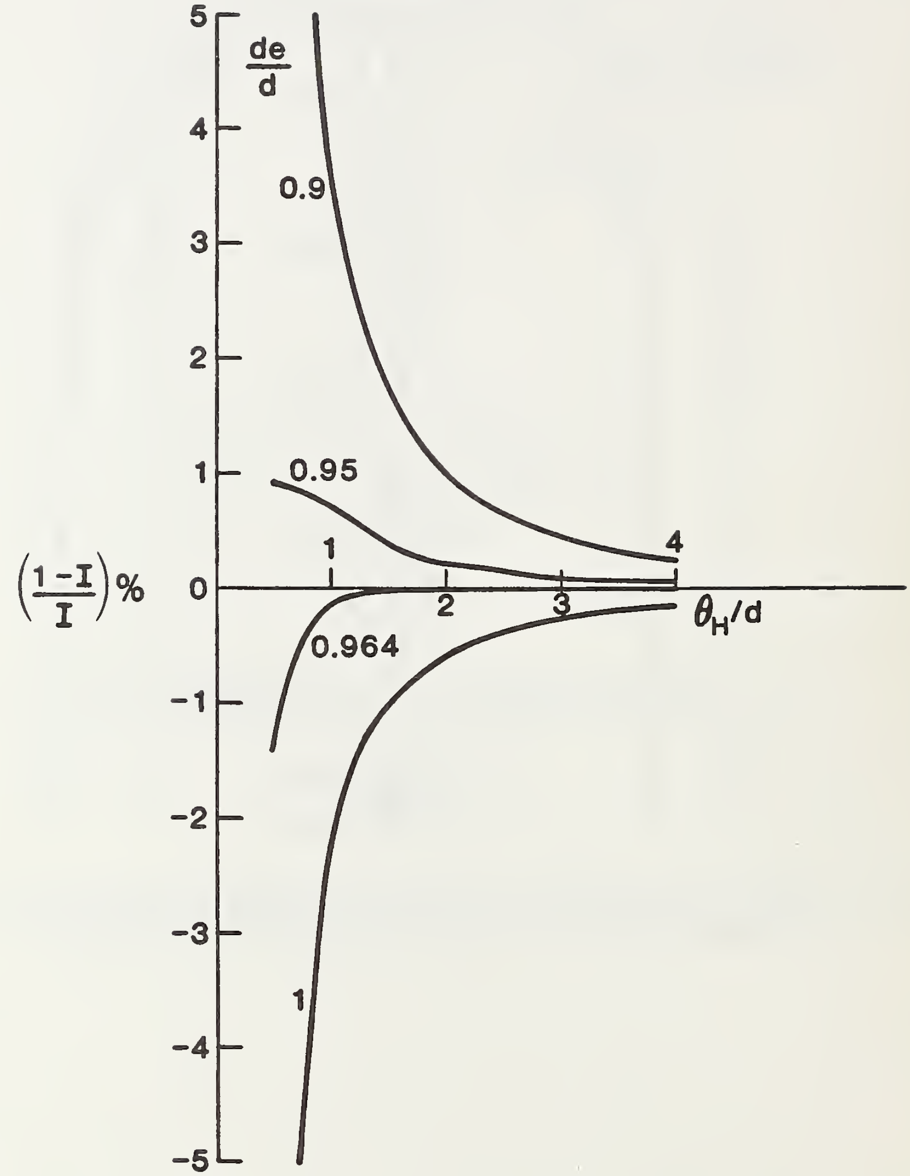

Figure 9. Error due to modeling k_2 as a disk versus θ_H/d at 168° and 9.375 GHz for various effective diameters.

figure shows that the error is quite sensitive to d_e. The object in choosing d_e is to minimize this error for θ_H/d greater than unity.

Figure 10 shows the error at 10 GHz for various lunar phases. Since the error for 45° is the largest, the d_e minimizing the error for this phase will automatically minimize the error at other phases. Figure 11 shows the results where a d_e of 0.965d produces the least error for θ_H/d above unity.

The above procedure was repeated at 5.5 and 1 GHz. An average of the three resulting diameters was taken as the effective diameter for the 1 to 10 GHz frequency range. The result of using this average diameter for the three frequencies is shown in figure 12. It is clear from the figure that the average diameter produces an error of less than 0.07 percent for the desired range of θ_H/d. This diameter, 0.964d, is then used in calculating the lunar shape factor with the disk model and leads to a value of x^2 given by

$$x^2 = 0.6441\ (d/\theta_H)^2. \qquad \text{(C10)}$$

An attempt was made to determine the error at 9.375 GHz from using the model contours (eq (C4)) instead of the actual contours from the literature [28]. The two contours differ mostly towards the lunar limb. To make the error calculations simpler, both the model and actual contours were approximated by a circularly symmetric fitting function of the form $(\cos \gamma')^n$. γ' is the angle between the earth-moon axis and the lunar latitude (see figure 6). When the model and actual contours were fit by this function, there resulted exponents (n) with values of 0.118 and 0.151, respectively. The error was then defined as $(k_2 - k_2')/k_2'$, where k_2 and k_2' are the shape factors calculated from the second factor in eq (C3) for the model and actual contours, respectively. The result, as a function of the ratio of HPBW to apparant lunar diameter, is shown in figure 13 with a maximum 0.25 percent for the ratio greater than unity.

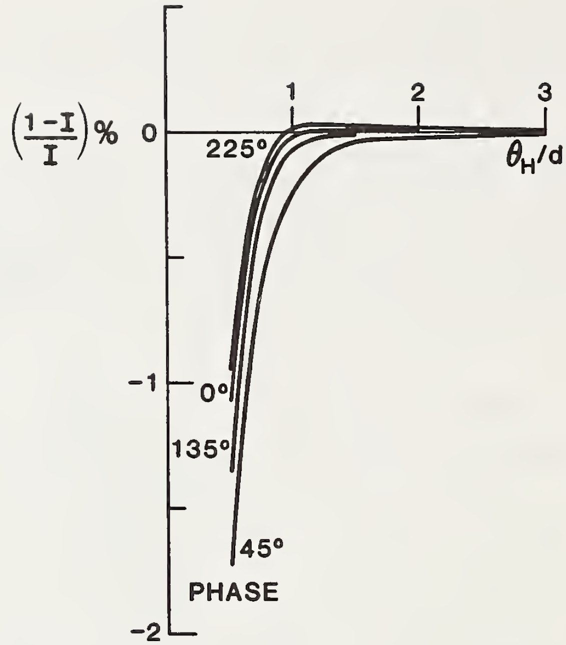

Figure 10. Error due to modeling k_2 as a disk versus θ_H/d at 10 GHz for an effective diameter of 0.965d and various phase angles.

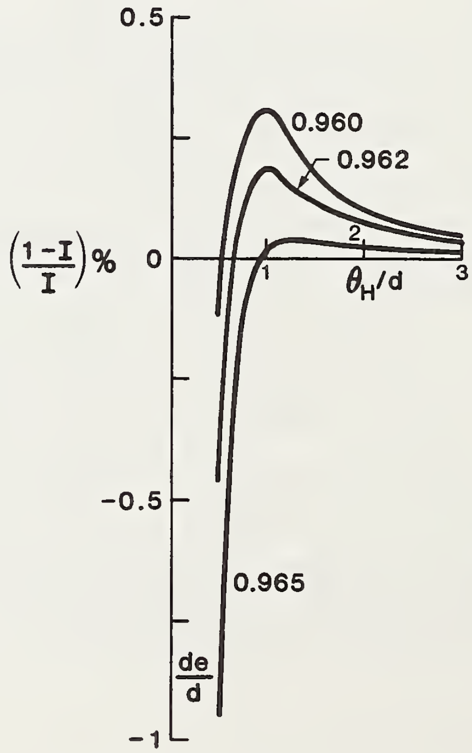

Figure 11. Error due to modeling k_2 as a disk versus θ_H/d at 45° and 10 GHz for various effective diameters.

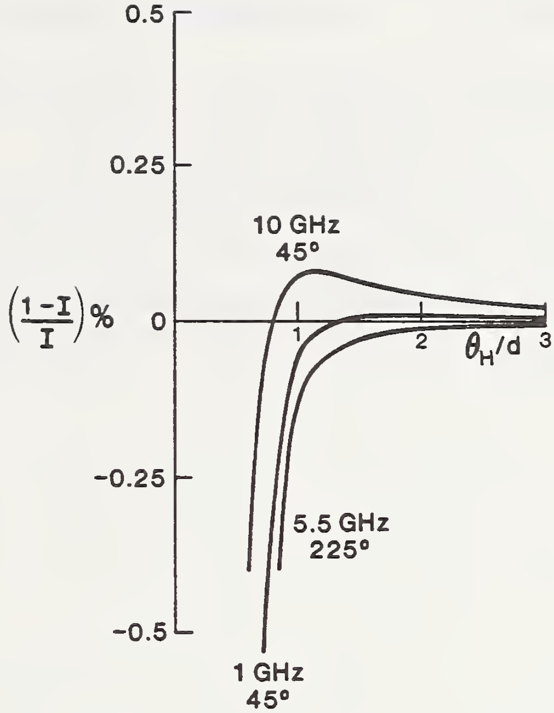

Figure 12. Error due to modeling k_2 as a disk versus θ_h/d for an effective diameter of 0.964d for various frequencies and phase angles.

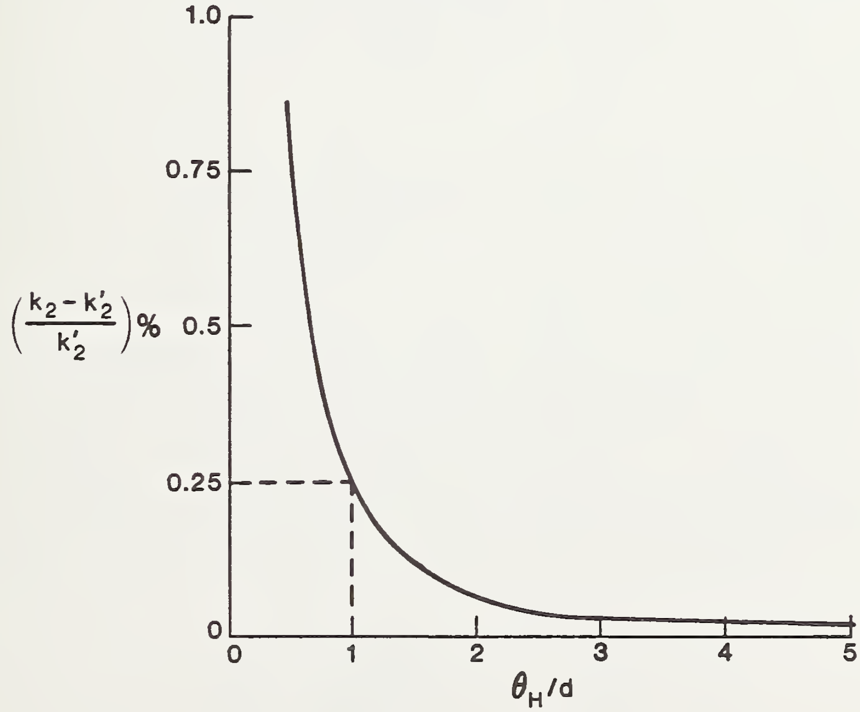

Figure 13. Model contour error versus θ_H/d for k_2 at 9.375 GHz.

Combining the errors due to I and the model contours results in

$$k_2 = \frac{1 - e^{-x^2}}{x^2} \pm 0.07\% \pm 0.25\% \qquad \text{(C11)}$$

where the second and third terms are the maximum errors in k_2 due to I and the model contours respectively.

APPENDIX D

AN EXPRESSION FOR THE AVERAGE BRIGHTNESS TEMPERATURE

Equation (C4) in Appendix C for the brightness temperature of the lunar surface is an approximation in which terms containing higher harmonics in the phase ϕ have been dropped. These deleted terms lead to higher terms in the average brightness temperature of eq (A10) which, for three harmonics, may be written as [22]

$$\bar{T} = \bar{T}_o - \bar{T}_1 \cos(\phi - \phi_1) + \bar{T}_2 \cos(2\phi - \phi_3)$$

$$+ \bar{T}_3 \cos(3\phi - \phi_3). \tag{D1}$$

The maximum relative error from dropping the second and third harmonics is

$$\frac{\Delta \bar{T}}{\bar{T}} = \left(\frac{\bar{T}_1}{\bar{T}_o}\right)\left(\frac{\bar{T}_2}{\bar{T}_1} + \frac{\bar{T}_3}{\bar{T}_1}\right) . \tag{D2}$$

This error increases with frequency, ultimately limiting the accuracy of the flux calculation. The maximum frequency of interest in the NBS system is 10 GHz and the error will be estimated at this frequency. From figure 2, the ratio $\bar{T}_1/\bar{T}_o$ is 0.07 at 10 GHz. At 75 GHz [22], the ratio $\bar{T}_2/\bar{T}_1$ and $\bar{T}_3/\bar{T}_1$ are 0.08 and 0.01 respectively. Assuming that these last two ratios can be scaled in frequency like the center-of-the-moon values shown in figure 4, the ratios at 10 GHz decrease to 0.022 and 0.003 respectively. Inserting these values into eq (D2) shows a total error of 0.18 percent for dropping the higher harmonic terms. Thus, below 10 GHz, eq (D1) can be written as [22, 27]

$$\bar{T} = \bar{T}_o \left[1 - \left(\frac{\bar{T}_1}{\bar{T}_o}\right)\cos(\phi - \Psi)\right] \pm 0.18\% . \tag{D3}$$

NBS-114A (REV. 2-80)

U.S. DEPT. OF COMM. BIBLIOGRAPHIC DATA SHEET (See instructions)	1. PUBLICATION OR REPORT NO. NBS TN-1073	2. Performing Organ. Report No.	3. Publication Date February 1984

4. TITLE AND SUBTITLE

An Error Analysis for the Use of Presently Available Lunar Radio Flux Data in Broadbeam Antenna-System Measurements

5. AUTHOR(S)

William C. Daywitt

6. PERFORMING ORGANIZATION (If joint or other than NBS, see instructions)

NATIONAL BUREAU OF STANDARDS
DEPARTMENT OF COMMERCE
WASHINGTON, D.C. 20234

7. Contract/Grant No.

8. Type of Report & Period Covered

9. SPONSORING ORGANIZATION NAME AND COMPLETE ADDRESS (Street, City, State, ZIP)

10. SUPPLEMENTARY NOTES

☐ Document describes a computer program; SF-185, FIPS Software Summary, is attached.

11. ABSTRACT (A 200-word or less factual summary of most significant information. If document includes a significant bibliography or literature survey, mention it here)

Simple, precise expressions for lunar diameter, average brightness temperature, flux density, and shape factor are presented. An analysis of the relationship between these parameters and corresponding errors are included. For broadbeam (HPBW>d) antennas, results show that flux density and shape factor can be determined with errors less than 13 percent and 0.4 percent respectively at frequencies below 10 GHz. Extension of the analysis to higher frequencies is indicated.

12. KEY WORDS (Six to twelve entries; alphabetical order; capitalize only proper names; and separate key words by semicolons)

antenna temperature; error analysis; G/T; lunar flux density; shape factor

13. AVAILABILITY

[X] Unlimited
☐ For Official Distribution. Do Not Release to NTIS
[X] Order From Superintendent of Documents, U.S. Government Printing Office, Washington, D.C. 20402.
☐ Order From National Technical Information Service (NTIS), Springfield, VA. 22161

14. NO. OF PRINTED PAGES

35

15. Price

USCOMM-DC 6043-P80

☆ U.S. GOVERNMENT PRINTING OFFICE: 1984—778-312/9198 REGION NO. 8

NBS TECHNICAL PUBLICATIONS

PERIODICALS

JOURNAL OF RESEARCH—The Journal of Research of the National Bureau of Standards reports NBS research and development in those disciplines of the physical and engineering sciences in which the Bureau is active. These include physics, chemistry, engineering, mathematics, and computer sciences. Papers cover a broad range of subjects, with major emphasis on measurement methodology and the basic technology underlying standardization. Also included from time to time are survey articles on topics closely related to the Bureau's technical and scientific programs. As a special service to subscribers each issue contains complete citations to all recent Bureau publications in both NBS and non-NBS media. Issued six times a year. Annual subscription: domestic \$18; foreign \$22.50. Single copy, \$5.50 domestic; \$6.90 foreign.

NONPERIODICALS

Monographs—Major contributions to the technical literature on various subjects related to the Bureau's scientific and technical activities.

Handbooks—Recommended codes of engineering and industrial practice (including safety codes) developed in cooperation with interested industries, professional organizations, and regulatory bodies.

Special Publications—Include proceedings of conferences sponsored by NBS, NBS annual reports, and other special publications appropriate to this grouping such as wall charts, pocket cards, and bibliographies.

Applied Mathematics Series—Mathematical tables, manuals, and studies of special interest to physicists, engineers, chemists, biologists, mathematicians, computer programmers, and others engaged in scientific and technical work.

National Standard Reference Data Series—Provides quantitative data on the physical and chemical properties of materials, compiled from the world's literature and critically evaluated. Developed under a worldwide program coordinated by NBS under the authority of the National Standard Data Act (Public Law 90-396).

NOTE: The principal publication outlet for the foregoing data is the Journal of Physical and Chemical Reference Data (JPCRD) published quarterly for NBS by the American Chemical Society (ACS) and the American Institute of Physics (AIP). Subscriptions, reprints, and supplements available from ACS, 1155 Sixteenth St., NW, Washington, DC 20056.

Building Science Series—Disseminates technical information developed at the Bureau on building materials, components, systems, and whole structures. The series presents research results, test methods, and performance criteria related to the structural and environmental functions and the durability and safety characteristics of building elements and systems.

Technical Notes—Studies or reports which are complete in themselves but restrictive in their treatment of a subject. Analogous to monographs but not so comprehensive in scope or definitive in treatment of the subject area. Often serve as a vehicle for final reports of work performed at NBS under the sponsorship of other government agencies.

Voluntary Product Standards—Developed under procedures published by the Department of Commerce in Part 10, Title 15, of the Code of Federal Regulations. The standards establish nationally recognized requirements for products, and provide all concerned interests with a basis for common understanding of the characteristics of the products. NBS administers this program as a supplement to the activities of the private sector standardizing organizations.

Consumer Information Series—Practical information, based on NBS research and experience, covering areas of interest to the consumer. Easily understandable language and illustrations provide useful background knowledge for shopping in today's technological marketplace.

Order the **above** *NBS publications from: Superintendent of Documents, Government Printing Office, Washington, DC 20402.*

Order the **following** *NBS publications—FIPS and NBSIR's—from the National Technical Information Service, Springfield, VA 22161.*

Federal Information Processing Standards Publications (FIPS PUB)—Publications in this series collectively constitute the Federal Information Processing Standards Register. The Register serves as the official source of information in the Federal Government regarding standards issued by NBS pursuant to the Federal Property and Administrative Services Act of 1949 as amended, Public Law 89-306 (79 Stat. 1127), and as implemented by Executive Order 11717 (38 FR 12315, dated May 11, 1973) and Part 6 of Title 15 CFR (Code of Federal Regulations).

NBS Interagency Reports (NBSIR)—A special series of interim or final reports on work performed by NBS for outside sponsors (both government and non-government). In general, initial distribution is handled by the sponsor; public distribution is by the National Technical Information Service, Springfield, VA 22161, in paper copy or microfiche form.

U.S. Department of Commerce
National Bureau of Standards

Washington, D.C. 20234
Official Business
Penalty for Private Use $300

U.S.MAIL

POSTAGE AND FEES PAID
U.S. DEPARTMENT OF COMMERCE
COM-215

FIRST CLASS